Journal of Molecular Structure 1245 (2021) 131057

Contents lists available at ScienceDirect

Journal of Molecular Structure

journal homepage: www.elsevier.com/locate/molstr

# Solvent induced distortion in a square planar copper(II) complex containing an azo-functionalized Schiff base: Synthesis, crystal structure, *in-vitro* fungicidal and anti-proliferative, and catecholase activity

Subham Mukherjee[a], Chanchal Kumar Pal[a], Muddukrishnaiah Kotakonda[b], Mayank Joshi[c], Madhusudan Shit[d], Prasanta Ghosh[e], Angshuman Roy Choudhury[c], Bhaskar Biswas[a,*]

[a] Department of Chemistry, University of North Bengal, Darjeeling-734013, India
[b] Department of Technology, Anna University, Chennai 600025, India
[c] Department of Chemical Sciences, Indian Institute of Science Education and Research, Mohali, Sector 81, Knowledge City, S. A. S. Nagar, Manauli PO, Mohali, Punjab 140306, India
[d] Department of Chemistry, Dinabandhu Andrews College, Kolkata 700084, India
[e] Department of Chemistry, Ramakrishna Mission Residential College, Kolkata 700103, India

ARTICLE INFO

*Article history:*
Received 19 April 2021
Revised 12 June 2021
Accepted 5 July 2021
Available online 10 July 2021

*Keywords:*
Copper(II)
Electrochemical analysis
Catechol oxidation activity
Schiff base
X-ray structure
Antifungal property
Antiproliferative activity

ABSTRACT

This research work reports the synthesis, single crystal X-ray structure, catechol oxidation, fungicidal and antiproliferative activity of a newly synthesized copper(II) complex, $[Cu(\mathbf{L})_2]H_2O \cdot CH_3OH$ (**1**) containing an azo-functionalized Schiff base, H**L** = 2-methoxy-6-((Z)-((4-((E)-phenyldiazenyl)phenyl)imino)methyl)phenol. The crystal structure analysis reveals that the Cu(II) centre exists in a highly distorted square planar geometry. The crystallize water and methanol form a strong intermolecular association through H-bonding. More importantly, the H atoms of the lattice water interact with the O atoms of ligand units leading to 5- and 6-membered cycles through the H-bonding network and distort the square planar geometry. The copper(II) complex has emerged as a bioinspired catalyst in the oxidative transformation of 3,5-di-*tert*-butylcatechol (DTBC) to o-benzoquinone in methanol with a high turnover number, $4.75 \times 10^2$ $h^{-1}$. Electrochemical analysis of the copper(II) complex in presence of DTBC recommends the generation of catechol/o-benzosemiquinone redox couple in the course of oxidation. The EPR spectral analysis of **1** in presence of DTBC was found silent and suggested the antiferromagnetic interaction between copper centre and benzosemiquinone species. The copper(II) complex turns out to be a potential fungicidal agent against clinical *candida albicans* and scanning electron microscope studies confirm the destruction of the fungal cell membrane with the deposition of copper. The $IC_{50}$ value of the copper complex was determined as 15 μg/mL which suggests the excellent antiproliferative potency of the synthetic compound against the breast cancer cell lines, MCF-7.



## 1. Introduction

Nowadays, azo-functionalised Schiff bases grab special attention for their unique and versatile structural and functional properties [1-3]. Generally, azo-functionalised compounds are widely used in dye and pigment industries [4,5]. Besides that azo compounds exhibit remarkable importance in the medicinal and pharmaceutical field including biological sciences [6-8]. These compounds show important electronic reversibility in photo-isomerisation processes and they are employed to a greater extent in the development of functional materials, optical computing, and coordination compounds [9-12]. Azo-functionalized Schiff bases form stable coordination compounds with interesting structural and functional properties [13]. amongst the various coordination compounds, copper(II) complexes have been paid substantial attention for their stability in an aerobic environment, good reactivity in solutions and the interesting flexible geometry [14-20]. Being a d9 system, copper(II) ion undergoes Jahn-Teller distortion and imposes a dis-

* Corresponding author.
*E-mail address:* bhaskarbiswas@nbu.ac.in (B. Biswas).

https://doi.org/10.1016/j.molstruc.2021.131057
0022-2860/

tortion in coordination geometries which facilitates the catalytic routes for different organic transformations [21-23].

The copper complexes mediated catalytic transformation of organic substrates in molecular oxygen environment increase exponentially using oxygen a sink of electrons (oxidase activity) as well incorporating oxygen atoms the product (oxygenase activity) or both [24-27]. In the biological world, copper ions in the coordination of various bio-ligands exist in the functional core of different metalloproteins [28-30]. At present different scientific groups are actively engrossed in the catalytic oxidations of organic substrates based on synthetic copper(II) based coordination compounds [31-34]. In light of a better understanding of metalloenzymes mediated biological oxidation and the emergence of novel antibiotics with potential resistance, it is of great importance to design novel antibiotics, which would destroy the lipid layer as well as the cell membrane of the pathogen with high selectivity [35,36]. In this perspective, copper-based coordination compounds hold a great promise to provide future alternatives to the existed antibiotics [37,38]. In the context of newly designed copper(II) complexes with high catalytic activities and potential therapeutic values, this research study describes the synthesis, structural characterization and catalytic catecholase activity of a newly synthesized square planar copper(II)-Schiff base complex. The fungicidal property against *candida albicans* and the antitumor activity towards the breast cancer MCF-7 cell lines has also been delineated.

## 2. Experimental

### 2.1. Preparation of the SCHIFF base and copper(II) complex

*(a) Chemicals, solvents and starting materials*

Highly pure 2-hydroxy-3-methoxybenzaldehyde (Alfa Aeser, UK), aniline (Merck, India), copper acetate monohydrate (Thomas Baker, India) and other reagents were purchased from respective suppliers. All the reagents and chemicals were of analytical grade. The solvents of spectroscopic grade were used to study the bio-inspired oxidation of catechol.

*(b) Synthesis of the Schiff base and copper(II) complex*

4-aminoazobenzene was prepared by using a previously reported well-established synthetic procedure [39]. 2-hydroxy-3-methoxy benzaldehyde (1.52 g, 10 mmol) was condensed with 4-aminoazobenzene (1.97 g, 10 mmol) under reflux for 8 hr in EtOH. The Schiff base was extracted as a reddish-orange crystalline product and dried in a vacuum desiccator.

Then, the yellowish brown coloured gummy product was extracted and stored *in vaccuo* over $CaCl_2$ for use. Yield: 0.317 g (~90.8%). Anal. Calc. for $C_{20}H_{17}N_3O_2$ (H**L**): C, 72.49; H, 5.17; N, 12.68; Found: C, 72.53; H, 5.20; N, 12.75. IR (KBr, $cm^{-1}$; Fig. S1): 3446 ($\nu_{OH2}$), 1618, 1593 ($\nu_{C=N}$), 1468 ($\nu_{N=N}$), 1260 ($\nu_{Ph\text{-}O}$); UV–Vis ($\lambda_{max}$, nm; Fig. S2): 224, 356; $^1$H NMR ($\delta$ ppm, 400 Mz, $CDCl_3$; Fig. S3) $\delta$ = 12.90 (s, 1H), 9.06 (s, 1H), 6.91–8.04 (Ar-H, 12H), 3.88 (s, 3H) ppm. $^{13}$C NMR (400 MHz,$CDCl_3$; Fig. S4): 206.9,192.4 (C-N=N-C); 164.90 (HC=N); 153.31,152.91,151.31,150.84(Ar-OH);148.85,143.27(Ar-N=C);131.98,129.94,125.60, 124.42, 123.0,122.94,120.57,119.78,118.0,116.40,113.84(Ar-C); 56.50, 40.55, 39.93,31.10 (–$OCH_3$).

The copper(II) complex containing azo-functionalized Schiff base was synthesized through the reaction of $Cu(OAc)_2$ (0.199 g, 1 mmol) with HL (0.69 g, 2 mmol) in MeOH-DCM solvent mixture. The reaction solution turned instantly to deep brown upon dropwise addition of $Cu(OAc)_2$ to HL and the total solution was stirring for 30 mins. The resultant solution was filtered and kept for slow evaporation. After a week, a green crystalline product of the copper complex was separated. The compound was dried over silica gel.

Yield of **1**: 0.775 g (~86.4%) Anal. calc. for $C_{41}H_{38}N_6O_6Cu$ (**1**): C, 63.60; H, 4.95; N, 10.85; Found: C, 63.65; H, 4.91; N, 10.89. IR (KBr pellet, $cm^{-1}$; Fig. S5): 3379 ($\nu_{OH}$), 1616,1581 ($\nu_{C=N}$), 1437 ($\nu_{N=N}$), 1252 ($\nu_{Ph\text{-}O}$); UV–Vis ($1 \times 10^{-4}$ M, $\lambda_{max}$(abs), nm, MeOH; Fig. S2): 230, 346.

### 2.2. Physical measurements

FTIR-8400S SHIMADZU spectrometer (Shimadzu, Kyoto, Japan) was employed to record IR spectra (KBr) of Schiff base and **1** ranging 400–3600 $cm^{-1}$. $^1$H and $^{13}$C NMR spectra of the ligand (H**L**) were obtained on a Bruker Advance 400 MHz spectrometer (Bruker, Massachusetts, USA) in $CDCl_3$ at 298 K. Steady-state absorption and other spectral data were obtained on a JASCO V-730 UV–Vis spectrophotometer (Jasco, Tokyo, Japan). A Perkin Elmer 2400 CHN microanalyser (Perkin Elmer, Waltham, USA) was used to perform the elemental analysis. X-band EPR spectra were recorded on a Magnettech GmbH MiniScope MS400 spectrometer (equipped with temperature controller TC H03, Magnettech, Berlin, Germany), where the microwave frequency was measured with an FC400 frequency counter. The electroanalytical instrument, BASi Epsilon-EC was employed for recoding the cyclic voltammograms in $CH_2Cl_2$ solutions. The BASi platinum working electrode, platinum auxiliary electrode, Ag/AgCl reference electrode were used for the measurements. Field emission scanning microcopy images of the fungal species in presence and absence of the copper complex was recorded with JSM-IT800 FESEM, Japan.

### 2.3. Crystal structure determination and refinement

X-ray diffraction data of **1** were collected using a Rigaku XtaLAB Mini diffractometer equipped with Mercury 375R ($2 \times 2$ bin mode) CCD detector. The data were collected with a graphite monochromated Mo-K$\alpha$ radiation ($\lambda$=0.71073 Å) at 150 K using $\omega$ scans. The data were reduced using CrysAlisPro 1.171.39.7f [40] and the space group determination was done using Olex2. The structure was resolved by the dual space method using SHELXT-2015 [41] and refined by full-matrix least-squares procedures using the SHELXL-2015 [42] software package through the OLEX2 suite [43]. The observed $R_{int}$ is high as the crystals of the copper(II) complex weren't diffracted to a great extent. Further, as a d-block metal, copper absorbs x-ray sometimes leading to additional residual density around copper. This fact accounts for the presence of residual density around the copper ion in this structure.

### 2.4. Catecholase activity of the copper(II) complex (*1*)

The catecholase activity was examined by the treatment of $1 \times 10^{-4}$ M solution of Cu(II) complex with $1 \times 10^{-3}$ M of 3,5-di-*tert*-butylcatechol (DTBC) in methanol under an aerobic atmosphere. absorbence vs. wavelength (wavelength scans) of the solution was monitored through a spectrophotometer at a regular time interval of 8 minutes for ~1.6 h in the wavelength range from 300–600 nm [44-45]. All the experiments were performed under aerobic conditions at room temperature.

Kinetic experiments were also performed with a spectrophotometer to determine the efficiency of catalytic oxidation of DTBC by the Cu(II) complex in MeOH [44-45]. The kinetics of catalytic transformation of DTBC was performed following the initial rate method. The catalytic oxidation was monitored as a function of time on the growth of the o-quinone species at 398 nm [46]. 0.04 mL of the solution of copper complex with a constant concentration of 1 × 10–3 M was added to 2 mL solution of DTBC of a particular concentration (varying its concentration from $1 \times 10^{-3}$ M to $1 \times 10^{-2}$ M) to achieve the ultimate concentration as $1 \times 10^{-3}$ M. The conversion of DTBC to 3,5-di-*tert*-o-

butylquinone was monitored with time at a wavelength 398 nm (time scan) in MeOH [44-47]. To determine the dependence of rate on substrate concentration, kinetic analyses were performed in triplicate.

The involvement of aerobic oxygen in the oxidation of DTBC was examined by the presence of hydrogen peroxide following a reported procedure [47]. In the oxidation of DTBC in MeOH, $H_2SO_4$ was added to reach pH 2 of the solution. After a certain time, the water of equal volume was further supplied to stop the oxidation. The o-quinone species were isolated using DCM as an extractant. 10 % KI solution (1 mL) and 3% ammonium molybdate solution were added to the aqueous layer. The development of $I_3^-$ was monitored through a spectrophotometer to examine the formation of $I_3^-$ band ($\lambda_{max}$= 353 nm) which reveals the production of hydrogen peroxide in the course of catalytic oxidation.

*Fungicidal susceptibility studies*

The fungicidal activity of the copper complex was performed against clinical *candida albicans*.

*2.5.1. Clinical cultures and culture media*

The fungicidal property of the copper complex was tested against clinical *candida albicans*. The microbial cultures were procured from the government medical college from Tiruchirappalli, Tamil Nadu. Muller-Hinton agar media of Himedia Pvt., India was used for the media. The fungicidal activity was evaluated employing the Himedia zone reader.

*2.5.2. Inoculums preparation*

A 100µL of clinical *C. albicans* organisms was inoculated in 5.0 mL of sterile nutrient broth (NB) media, PDB (Potato dextrose broth) and incubated at 37 °C for 24 h. 200µL of the fresh culture of the *C. albicans* was dispensed into 30 mL sterile nutrient broth and incubated 24 h to standardize the culture to $10^8$ CFU/ml (colony forming units).

*2.5.3. Agar well diffusion method (Kirby-Bauer method)*

The fungicidal activity of the copper complex and a standard marketed drug (Fluconazole-100 mg/2 mL) was studied initially by using the agar well plate method. *C. albicans* inoculum was prepared by using sterile nutrient broth media. Mueller Hinton agar double strength media were made by autoclaving 0.760 g in 100 ml. Standardized inoculums inoculate the test microorganisms on the Mueller Hinton agar plates by using sterile cotton swabs. Four 8 mm diameter agar wells were prepared using sterile corkborer, and copper complex 0.1 ml (50 mg/ml) and 0.1 ml Fluocazole (10 mg/ml) were placed on agar well using micropipette under aseptic conditions. Sterile water was used as a negative control. Agar plates were incubated for 30 min at the refrigerator to diffuse the formulation into the agar, and finally, plates were incubated at 37°C for 24 h. Antifungal activity was evaluated by using the Himedia zone reader.

*Preparation of stock solutions for MIC was done following the equation 1.*

Weight of the powder (mg) =

$$\frac{\text{Volumeofsolution(mL)} \times \text{Concentration(mg/L)}}{\text{The potency of powder } (mg/g)} \quad (1)$$

*2.5.3. Determination of minimum inhibitory concentration (MIC) for copper complex against clinical C. albicans*

The method of micro-dilution was used to establish the antibacterial potential of the copper complex and respective controls. A spectrophotometer (OD595= 0.22) equivalent to $10^8$ CFU/mL used to fix the bacterial cultures to 0.22 optical density at 595 nm. Different concentrations of copper complex (100, 50, 25, 12.5, 6.25 mg/mL) and the standard drug, fluconazole (50, 25, 12.5, 6.25, 3.125, 1.5625 mg/mL) were added to the respective controls in 2.0 mL MIC tubes. $10^8$ CFU/ml 100 $\mu$L of the tested were added into each MIC test tube. MIC tubes were incubated overnight at 37 °C for 24 h.

*2.5.4. Antifungal activity of copper(II) complex using scanning electronic microscope*

To examine the mode of action of copper(II) complex on the fungal species, fungi cultures were obtained from MIC samples and centrifuged. Thereafter, the fungi cells were collected and sputter-coated with a thin layer of gold-palladium. The coated fungal cells were fixed on a glass coverslip and observed under a scanning electron microscope.

*2.6. Antiproliferative activity of the copper complex*

*2.6.1. Chemical and reagents for antitumor activity*

Dulbecco's Modified Eagle's Medium (DMEM), streptomycin, penicillin-G, L-glutamine, phosphate-buffered saline, (3-[4,5-dimethylthiazol-2-yl]-2,5-diphenyltetrazolium bromide; MTT), ethylene diamine tetraacetic acid (EDTA), ethanol, and dimethyl sulfoxide (DMSO) were purchased from Sigma Aldrich Chemicals Pvt. Ltd (India). All other chemicals were of analytical grade and purchased from Himedia Laboratories Pvt. Ltd. India.

*2.6.2. Cell culture maintenance*

Human breast cancer MCF-7 cell lines were procured from the cell repository of the National Centre for Cell Sciences (NCCS), Pune, India. DMEM was used for maintaining the cell line which was supplemented with 10% fetal Bovine Serum (FBS). The penicillin (100 $\mu$g/mL), and streptomycin (100 $\mu$g/mL) was added to the medium to prevent the microbial contamination. The medium constituting the cell lines was maintained in a humidified environment with 5% $CO_2$ at 37 °C.

*2.6.3. MTT assay*

The cytotoxicity of the copper complex on the breast cancer cell lines, MCF-7 was determined through 3-[4,5-dimethylthiazol-2-yl]-2,5-diphenyltetrazolium bromide (MTT) assay employing the method reported by Mosmann *et al* (1983).

50 mg of MTT dye was dissolved in 10 mL of PBS. After vortexing for 1 min, it was filtered through 0.45 microfilters. The bottle was wrapped with aluminium foil to prevent light, as MTT was light-sensitive. The preparation was stored at 4 °C.

Cell viability assay for MCF-7 viable cells was harvested and counted using a hemocytometer and diluted in DMEM medium to reach a density of $1 \times 10^4$ cells/mL which were seeded in 96 well plates for each well and incubated for 24 h to allow attachment. After MCF-7 cells treated with control and the containing different concentrations of copper complex 5 to 30 $\mu$g/ml were applied to each well. MCF-7cells were incubated at 37 °C in a humidified 95% air and 5% $CO_2$ incubator for 24 h. After incubation, the drug-containing cells wash with a fresh culture medium and the MTT (5 mg/ml in PBS) dye was added to each well, followed by incubated for another 4 h at 37 °C. The purple precipitated formazan formed was dissolved in 100 µl of concentrated DMSO and the cell viability was absorbence and measured 540 nm using a multi-well plate reader. The results were expressed at the percentage of stable cells to the control. The half-maximal inhibitory concentration ($IC_{50}$) values were calculated and the optimum doses were analysed at the different periods.

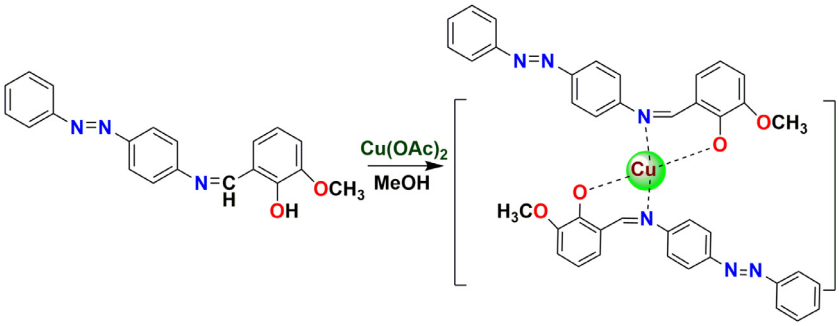


**Scheme 1.** Synthetic route for the copper(II) complex.

$$\text{Inhibitory of call proliferation}(\%) = \frac{\text{Mean absorbence of the control} - \text{Mean absorbense of the sample}}{\text{Mean absorbence of the control}} \times 10$$

The $IC_{50}$ values were determined from the dose-responsive curve of the copper complex. All experiments were performed at least three times in triplicate. The values are expressed as mean ± SD. The statistical comparisons were performed by one-way analysis of variance (ANOVA) followed by Duncan's Multiple Range Test (DMRT), using SPSS version 12.0 for windows (SPSS Inc. Chicago; http://www.spss.com). The values are considered statistically significant if the p-value was less than 0.05.

## 3. Results and discussion

### *3.1. Design, synthesis and formulation of the Schiff base (HL) and copper(II) complex (1)*

The azo-functionalized Schiff base (H**L**) was synthesized by a reaction between 4-aminoazobenzene and 2-hydroxy-3-methoxy benzaldehyde under refluxing conditions. The copper(II)-Schiff base complex was synthesized by reacting copper(II) acetate with H**L** in 1:2 mole ratio in a methanol medium. The synthetic procedure is shown in Scheme 1. Attempts were also made to develop the different structural composition of the copper(II)-Schiff base complex, perhaps we were unsuccessful to produce the different structure. Both the Schiff base and the copper(II) complex are soluble in polar solvents like methanol, ethanol, acetonitrile, chloroform etc.

### *3.2. Description of crystal structure and non-covalent interactions*

The crystal structural analysis reveals that the copper complex crystallizes in a monoclinic system with a $P2_1/c$ space group. The ORTEP diagram of the Cu(II) complex is displayed in Fig. 1. The crystallographic refinement parameter is summarized in Table 1 and bond angles, and bond distances are given in Table 2. The azo-functionalized Schiff base contains three donor centres in association with an azo group, however, during coordination two donor centres of one ligand unit coordinate with the copper(II) centre ion as a bidentate chelator. The copper(II) complex adopts two units of coordinated Schiff base and exists in a highly distorted square planar coordination geometry. The deviation of copper(II) centric average bond angles (∠L–M–L, 94.23) from the tetrahedral geometry is found larger while the average bond angles around copper(II) centre (∠L–M–L, 94.23) are closer to the average value of an ideal square planar geometry (Table 2). Therefore, bond angle measurements around the copper centre support the existence of a square planar geometry.

To understand the cause of distortion, the effect of solvate molecules and the presence of noncovalent interactions in the crystalline architectures of the copper complex were examined. It was observed that the crystallized water and methanol form a very strong intermolecular H-bonding network with the copper complex ranging from 1.91 Å to 2.11 Å (Fig. S6). Investigation of the self-assembly of the copper complex exhibits that methanol-

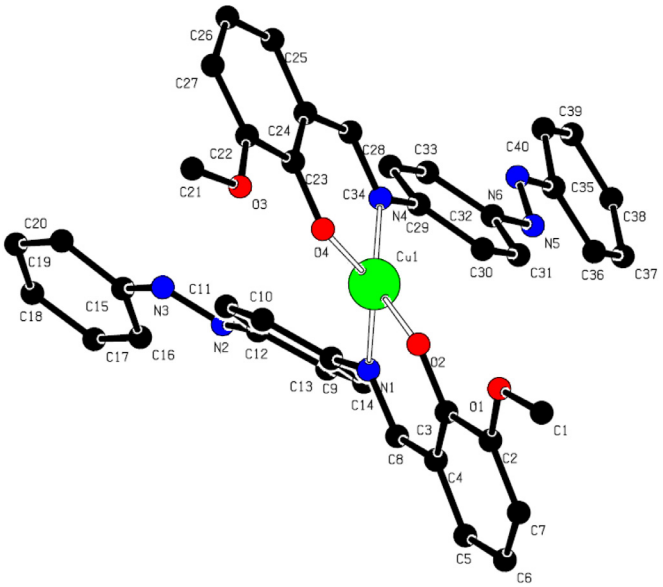


**Fig. 1.** Ball and stick drawing of the copper(II) complex with 30% probability. The hydrogen atoms and the solvent molecules are removed for clarity.

**Table 1**
Crystallographic data and structure refinement parameters for **1**.

| Parameters | 1 |
|---|---|
| Empirical formula | $C_{41}H_{38}N_6O_6Cu$ |
| Formula weight | 774.31 |
| Temperature (K) | 150 |
| Crystal system | Monoclinic |
| Space group | $P2_1/c$ |
| a (Å) | 16.104(2) |
| b (Å) | 18.584(2) |
| c (Å) | 13.265(2) |
| Volume (Å$^3$) | 3748.4(9) |
| Z | 4 |
| $\rho$ (gcm$^{-3}$) | 1.3721 |
| $\mu$ (mm$^{-1}$) | 0.639 |
| F (000) | 1612 |
| $R_{int}$ | 0.181 |
| $\theta$ ranges (°) | 2.6–25 |
| Number of unique reflections | 6579 |
| Total number of reflections | 32,338 |
| Final R indices | 0.0750, 0.2230 |
| Largest peak and hole (eA$^{\circ-3}$) | 1.00, -0.63 |

**Table 2**
Bond angles and bond distances value of Cu(II) complex.

| | | | |
|---|---|---|---|
| Bond distances (Å) | | | |
| Cu1 –O2 | 1.894(3) | Cu1- O4 | 1.890(3) |
| Cu1 –N1 | 1.985(3) | Cu1 - N4 | 1.978(3) |
| Bond angles (°) | | | |
| ∠O2-Cu1-O4 | 88.79(13) | ∠O4-Cu1-N1 | 145.64(14) |
| ∠O2-Cu1-N1 | 93.17(14) | ∠O4-Cu1-N4 | 94.78(13) |
| ∠O2 -Cu1-N4 | 150.08(14) | ∠N1-Cu1-N4 | 100.19(14) |

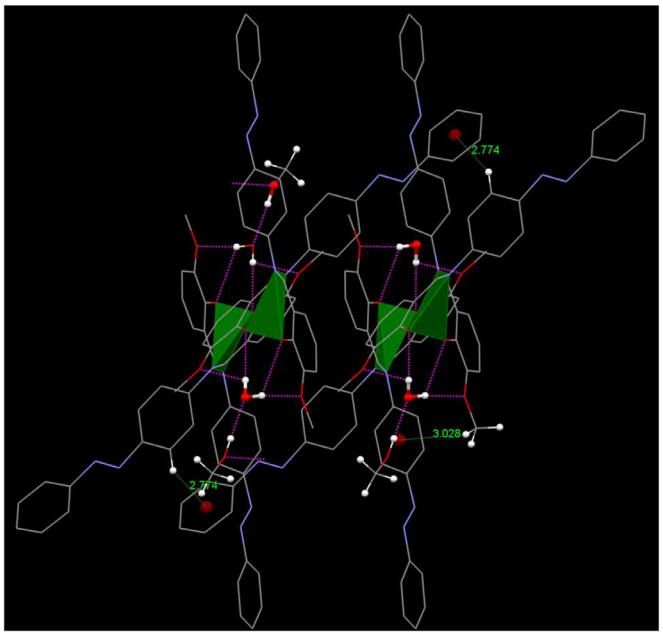


**Fig. 2.** OH (pink dash lines) and C–H···$\pi$ (green dashed lines) mediated formation of a supramolecular architecture for the copper(II) complex. (For interpretation of the references to colour in this figure legend, the reader is referred to the web version of this article.)

OH(H6A) acts as an acceptor towards the oxygen of water (O5) while the O5 atom behaves as a donor to develop a strong intermolecular association between the crystallized water and methanol molecules (Fig. S6). Furthermore, the hydrogen atoms of water (H5A and H5B) play a key role in causing a high distortion in the molecules. Two H-atoms of water strongly hold two units of azo-functionalized Schiff base separately through the strong intermolecular network (H5A···O3, 2.14 Å; H5A···O4, 2.45 Å; H5B···O1, 2.45 Å; H5B···O2, 2.11 Å, Fig. 2, Table S1). More captivatingly, the Hs of O5 in the crystallized water form two 5-member cyclic rings with the phenoxo-O and methoxy-O of the ligand units and as a result a 6-member cycle is also formed with the copper centre coordinated by the phenoxo-O (Fig. 2). This intermolecular H-bonded network amongst the crystallize solvate molecules and ligand units account for the cause of high distortion in the chelating ligands during coordination. It is further documented that for the involvement of strong intermolecular H-bonding in ligand units, the methoxy-O didn't coordinate with the copper centre.

A close look at the nature of non-covalent interactions suggests that the mononuclear copper(II) complex interacts with another complex unit through strong O···H and C–H···$\pi$ and seems to be a complex dimer (Fig. 2, Table S2). This complex dimer is further extended and stabilized through the intermolecular C–H···$\pi$ interactions between the azo-linked phenyl-C–H and the terminal centroid of the azo-linked phenyl ring. The H of the methyl group adds more stabilization energy to the complex dimer through another set of C–H···$\pi$ interactions in the crystalline phase (Fig. 2, Table S2).

The Hirshfeld surface analysis of the copper(II) complex over a definite $d_{norm}$ was calculated with Crystal Explorer software. The surface volume and area are calculated as 963.85 Å$^3$ and 687.91 Å$^2$. The red highlighted spots indicate the $d_{norm}$ area and present close non-covalent interactions in the copper complex with its surrounding molecules (Fig. S7). The contribution of each element in the non-covalent interactions is given in Table S3. The blue area in $d_{norm}$ cites important C–H···$\pi$ interactions between the azo-linked phenyl centroid with the H of C-attached to phenyl and methyl groups. The white denotes no interaction. The interactions in the copper(II) complex is displayed in Fingerprint plots (Fig. S8).

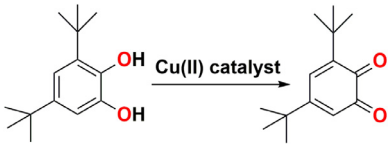


**Scheme 2.** Catalytic oxidation of DTBC to DTBQ.

### 3.3. Solution property of the Schiff base and copper(II) complex

The Schiff base exhibit characteristic electronic transitions at 224 and 356 nm while the copper(II) complex displayed the electronic bands at 230 and 346 nm in methanol at room temperature. The electronic bands at 224 and 365 nm in the Schiff base are assignable to the presence of $\pi \rightarrow \pi^*$ and charge transfer (CT) transitions respectively. The lower energetic electronic band at 346 nm gets blue-shifted in the complex and is attributed to the CT band from $PhO^- \rightarrow$ Cu(II) centre exhibited electronic bands at 238, 283 and 400 nm. The electronic spectra are displayed in Fig. S2. The appearance of the characteristic electronic bands for the Schiff base and copper complex are in good agreement with the previously reported values of electronic transitions [48,49]. The high resolution mass spectrum was recorded in methanol at room temperature to reveal the purity and homogeneity of copper complex in solution. The spectrum is displayed in Fig. S9. The mass spectrum shows a characteristic peak at 723.21 *m/z* which ensures the existence of the tetracoordinate copper(II) complex with its structural integrity and suggests the homogeneity of the compound in MeOH.

### 3.4. Catecholase activity of the copper(II) complex (*1*)

The catecholase activity of the copper(II) complex has been examined by considering 3,5-di-*tert*-butyl catechol (DTBC) as a model substrate. DTBC contains two bulky *t*-butyl substituents at the phenyl ring and helps to lower down the quinone-catechol reduction potential. The low quinone-catechol reduction potential facilitates the oxidation of catechol to the corresponding *o*-quinone, DTBQ under ambient reaction conditions (Scheme 2). It is well documented that DTBQ is quite stable in solution and displays a characteristic absorption peak at 401 nm in methanol [50].

The nature of changes of the spectral bands during the catalytic oxidation was monitored with a UV–Vis spectrophotometer for a period of 1.6 h (Fig. 3). The copper complex displays a characteristic electronic transition at 346 nm. Upon addition of the Cu(II) complex to the solution of DTBC, a new electronic band at 398 nm was started to develop with increasing absorbence (Fig. 3). The rise of the optical band at 398 nm is a definite sign of the oxidation of DTBC in MeOH [51,52]. The appearance of this new electronic band at 398 nm in the spectrophotometric scan is assignable to the production of the o-benzoquinone species in MeOH.

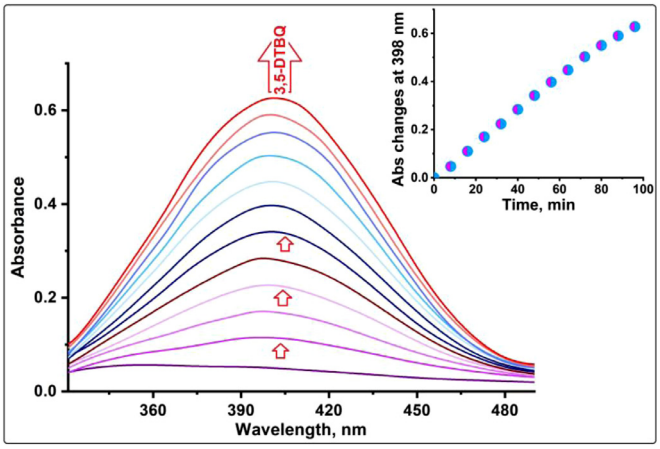


**Fig. 3.** Rise of a new electronic band at 398 nm upon addition of copper complex **1** to DTBC in MeOH with a time interval of 8 mins. Inset: Time vs absorbence plot at 398 nm.

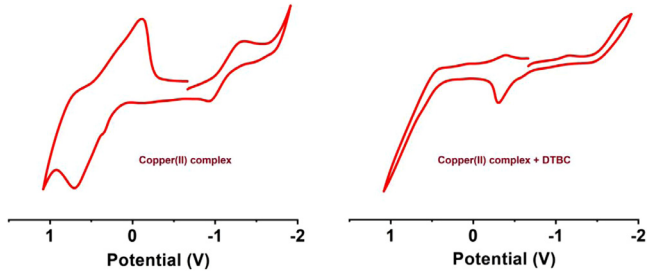


**Fig. 4. Left:** Cyclic voltammogram of the copper(II) complex **1** in $CH_2Cl_2$; **Right:** Cyclic voltammogram of copper(II) complex **1** in presence of DTBC under molecular oxygen atmosphere in $CH_2Cl_2$.

The kinetics for the catalytic oxidation of DTBC was studied to determine the catalytic performance of the copper(II) complex. The kinetic parameter of the catalytic oxidation of DTBC was evaluated employing the method of the initial rate. The growth of o-benzoquinone was monitored as a function of time with respect to 398 nm (Fig. S10) [53]. The nature of oxidation kinetics was examined by plotting the rate constants vs. concentration of DTBC and shown in Fig. S10. The first order saturation kinetics of the oxidation reaction seems to be suitable in the Michaelis–Menten model and can be expressed as the Eq. (2):

$$V = \frac{V\max[S]}{KM + [S]} \quad (2)$$

Where, $V$ indicates the rate of oxidation reaction, $K_m$ denotes the Michaelis-Mentenconstant, $V_{max}$ presents the maximum velocity of the reaction, and [$S$] is the concentration of the DTBC.

The values of kinetics parameters were determined from Michaelis–Menten equation as $V_{max}(MS^{-1}) = 1.32 \times 10^{-4}$; $K_M = 4.52 \times 10^{-3}$ [Std. Error for $V_{max}$ $(MS^{-1}) = 7.79 \times 10^{-5}$; Std. Error for $K_m$ (M)= $4.53 \times 10^{-4}$]. The catalytic efficiency for the catalytic oxidation of DTBC was determined as $k_{cat}/K_M = 1.05 \times 10^5$.

The redox activities of the copper complex and its activities toward the biomimetics of the catecholase activities were studied by electrochemical analysis in $CH_2Cl_2$ at 295 K. The redox behaviour of the copper complex was recorded using ferrocenium/ferrocene ($Fc^+$/Fc) reference under aerobic atmosphere. The cyclic voltammograms are illustrated in Fig. 4. The copper(II) complex exhibits a quasi-reversible cathodic wave at -1.13 V due to $Cu^{2+}/Cu^+$ redox species in solution. The anodic peak appears at +0.70 V due to phenoxide/phenoxide anion radical($O^-/O\bullet-$) redox couple and the peak at -0.11 V is for the deposition of copper. The catecholase activity was authenticated by the change in cyclic voltammograms of the copper complex in presence of DTBC in $CH_2Cl_2$ at 295 K. Cyclic voltammograms of the copper complex in presence of DTBC produces an anodic peak at -0.30 V perhaps the cathodic wave of $Cu^{2+}/Cu^+$ couple was disappeared. This peak is a definite sign of the oxidation of DTBC. Therefore, this peak is assignable to cat/sq redox couple (cat = catechol, sq = o-benzosemiquinone and isq = o-iminobenzosemiquinone). The disappearance of $Cu^{2+}/Cu^+$ peak indicates the involvement of $Cu^{2+}$ in the oxidation processes. This metal-mediated oxidation of DTBC was also authenticated by the EPR spectral analysis. The copper complex gives a four-line hyperfine structure at g = 2.13 due to $^{63,65}Cu$ in $CH_2Cl_2$ at 295 K (Fig. S11). However, in the presence of DTBC, the metal complex becomes EPR silent (Fig. S12). This is due to the antiferromagnetic coupling between the copper centre and semiquinone species. These experiments strongly support the metal-mediated oxidation of DTBC. Further, the fate of molecular oxygen in the oxidation of DTBC was examined through the production of hydrogen peroxide in solution [37,38]. An electronic band at $\lambda_{max}$ 353 nm confirmed the development of hydrogen peroxide in the course of catalytic oxidation and thereby, ensured the transformation of molecular oxygen to $H_2O_2$ in the catalytic oxidation of DTBC. Furthermore, the retention of structural identity of the copper(II) complex was confirmed in the catalytic oxidation of DTBC by measuring the UV–vis spectrum of the solution after separating the oxidation product. The solution containing the copper complex as catalyst produces similar kind of electronic bands at 233 and 350 nm (Fig. S13) as like the electronic bands of the original copper complex displayed in methanol and ensures the retention of structural identity in catalytic oxidation of DTBC. Therefore, based on the experimental outcomes, a plausible mechanistic cycle for the catalytic oxidation of DTBC may be proposed according to the following scheme 3. A comparison of catalytic oxidation of DTBC by this Cu(II) complex with some other reported Cu(II) complexes is furnished in Table 3 [51-54].

**Table 3**
Comparison of $k_{cat}$ ($h^{-1}$) values for catalytic oxidation of DTBC by reported copper(II) compounds and **1**.

| Complex | $k_{cat}$ ($h^{-1}$)(Solvent) | CCDC No | Ref |
|---|---|---|---|
| $[Cu(dpa)_2NCS]_2$ | 4788 ($CH_3OH$) | 1456703 | [51] |
| $[Cu(dpa)_2(NCS)_2](ClO4)_2$ | | | |
| $[Cu_2(L^{1*}SSL^{1*})](BF_4)_4$ | $6.90 \times 10^3$($CH_3CN$) | - | [52] |
| $[Cu(phen)(OH_2)_2(NO_3)](NO_3)$ | $3.91 \times 10^3$($CH_3OH$) | 1061531 | [53] |
| $[Cu(2,2^{z}bpy)Cl_2]$ | $2.08 \times 10^3$($CH_3OH$) | 1524681 | [45c] |
| $[Cu(2,2^{z}bpy)_2(OAc)]^+$ | $1.83 \times 10^3$ ($CH_3OH$) | 1513638 | [54] |
| $[Cu(\mathbf{L})_2]$ | $4.75 \times 10^2$ ($CH_3OH$) | 2046277 | This work |

### 3.6. Fungicidal activity of the Cu(II)-Schiff base complex

The fungicidal activity of the copper complex was assessed with a well diffusion method against the fungi *candida albicans*. The results of the inhibition zone diameters are shown in Table S4. The antifungal efficiency for the Cu(II) complex was determined by calculating MIC on *candida albicans*. The minimum inhibitory concentration *(MIC) value was estimated as* 230 μg/mL for the *copper(II) complex.* Scientific literature suggest that the Cu(II) complex is quite competent to inhibit the growth of *candida albicans*. Under a similar experimental condition, the standard fluconazole shows the MIC value of 6.25 μg/mL (Table S5). The MIC value suggests a good fungicidal potency for the inhibition of the growth of *c. albicans* fungal species under experimental conditions. To understand the origin of fungicidal activity of the copper(II) complex, field emission *scanning* electron microscopy (FESEM) image

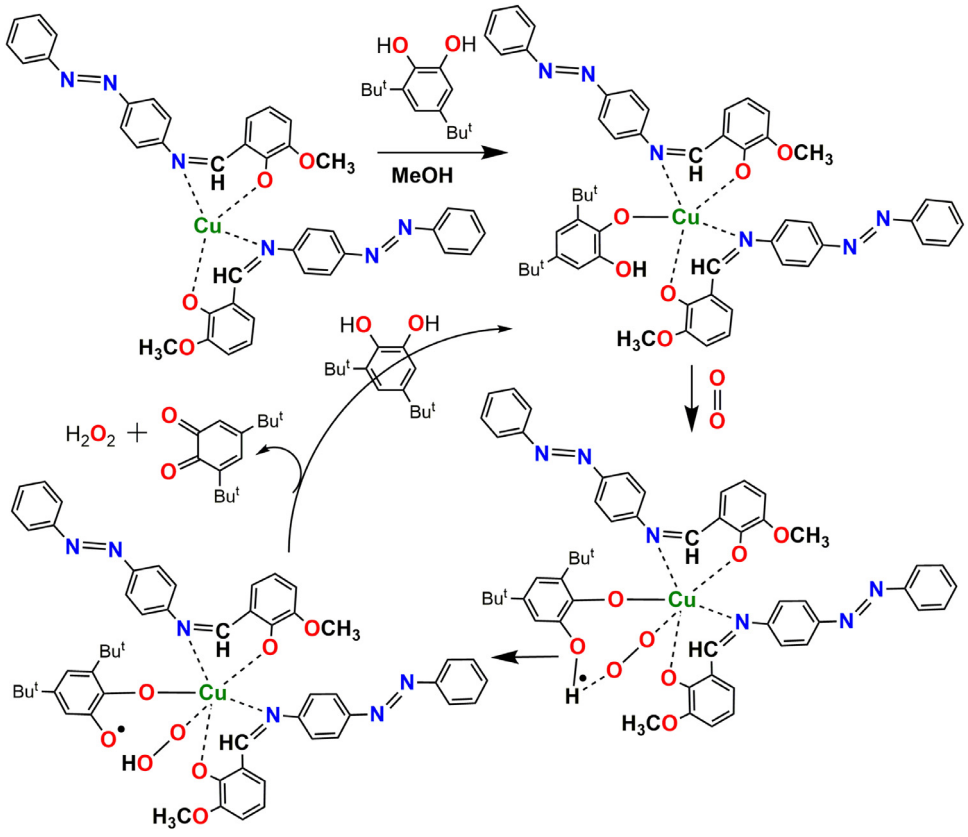


**Scheme 3.** Plausible mechanistic cycle for catecholase activity of the copper complex.

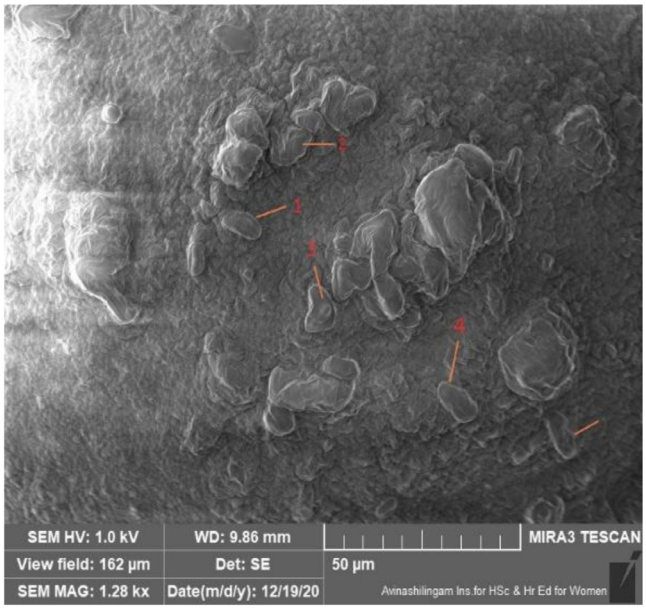


**Fig. 5.** Morphological changes in *candida albicans* upon treated with the Cu(II) complex.

was recorded for the *candida albicans upon treatment with copper(II) complex.* The recorded SEM micrographs of *candida albicans* cells are shown in *Fig. 5*. Commonly, the *candida albicans* fungal species was found as nearly spherical-shaped cell morphology with smooth and intact cell walls. It is well observed that the number of *candida albicans* was remarkably decreased, and clusterized. The cell walls of the fungal species *candida albicans* became damaged and shrinked upon the interaction of the Cu(II) complex with the fungi [55,56]. Most captivatingly, the presence of elemental copper was detected on the cell wall of *candida albicans* through the energy dispersive X-ray spectroscopy (Fig. S14) and is shown as the orange coloured mark in Fig. 5. Truly, the presence of elemental copper on cell wall is a remarkable phenomenon to report and in very limited cases, such type of observation was noted.

### 3.7. Antiproliferative activity of the Cu(II)-Schiff base complex

MTT assay was employed to determine the cytotoxic effect of the copper(II) complex on MCF-7 cell lines. The breast cancer cell lines, MCF-7 were treated with the copper(II) complex in a dose dependant manner varying the concentration 5 to 30 µg per ml for 24 h. The results are expressed as a percentage of the control value in presenting as a cell cytotoxicity ratio for MCF-7 cells and displayed in Fig. 6. The $IC_{50}$ value for the copper complex was determined as 15 µg/mL against MCF-7 cells for 24 h. It is well documented that (3-[4,5-dimethylthiazol-2-yl]-2,5-diphenyltetrazolium bromide is a water soluble tetrazolium salt yielding a yellowish solution when prepared in media. The yellow coloured MTT is reduced by mitochondrial dehydrogenase of viable cells yielding a measurable purple formation product. The viable cells consist of NADPH-dependant reductase and reduce the MTT reagent to formazon with the development of deep purple formazon species. Thereafter, the absorbence of formazon solution was measured by plate reader to examine the cytotoxic effects of the copper complex. The induced morphological changes in MCF-7 cells by Cu(II) complex (Fig. 7) leads to the shrinkage, detachment and membrane blebbing which suggests the high anti-proliferative potency of the copper complex.

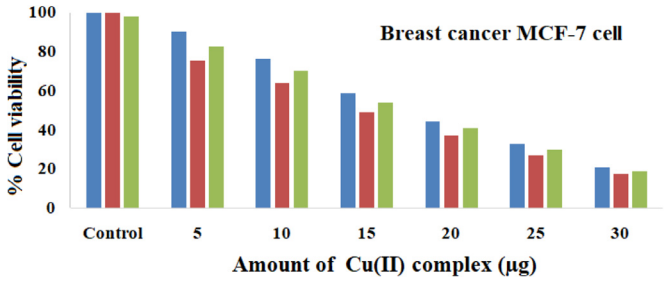


**Fig. 6.** Cellular viability of breast cancer cell lines, MCF-7 cells treated with copper(II) complex in a dose dependant manner for 24 h employing MTT assay.

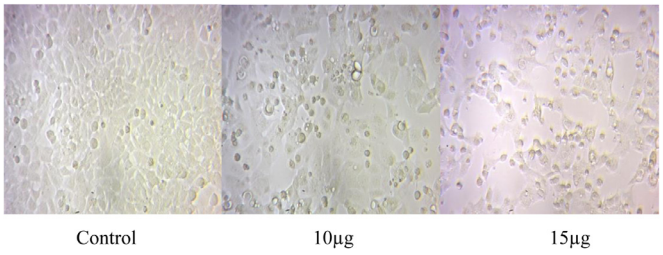


**Fig. 7.** Photomicrograph (40 ×) represents morphological changes in MCF-7 cells such as shrinkage, detachment, membrane blebbing and distorted shape induced by Cu(II) complex (10 and 15 µg/mL for 24 h) as compared with control. Control cells showed normal intact cell morphology and their images were captured by light microscope. (For interpretation of the references to colour in this figure legend, the reader is referred to the web version of this article.)

In true sense, the introduction of the azo-functionalized copper(II)-Schiff base complex helps to develop reactive oxygen species (ROS) in the lipid peroxidase in MCF-7 cells. Consequently, the redox active copper complex generates more reactive free radicals which involve in the destruction of membrane lipid of MCF-7 cells. This phenomenon accounts for the detachment and shrinkage of the normal cells and increases the apoptosis of MCF-7 cells. This observation is also supported by previously reported anti-tumour activities induced by copper complexes [55,56].

## 4. Conclusions

This research work deals with the synthesis, crystal structure, bio-mimics of catecholase, antifungal and antitumor activity of a newly designed copper(II) complex containing an azo-functionalized Schiff base. The copper(II) centre adopts a distorted square planar geometry. The strong association of lattice water with the ligand units through very strong intermolecular H-bonding interaction induces a large distortion in the square planar complex. The copper(II) complex exhibits a good catalytic activity with a high turnover number, $4.75 \times 10^2$ $h^{-1}$ towards the catalytic oxidation of DTBC in methanol. Electrochemical, EPR and spectrophotometric spectral studies of the copper(II) complex in presence of DTBC suggest the copper(II) mediation catalytic oxidation of DTBC. The copper(II) complex turns out to be a potential fungicidal agent against clinical *candida albicans* and scanning electron microscope studies confirm the destruction of the fungal cell membrane with the deposition of copper. In vitro study of cytotoxicity of the copper complex towards the breast cancer, MCF-7 cell lines account for its excellent antiproliferative potency at $IC_{50}$ value, 15 µg/mL for 24 h. The synthesis of azo-functionalized Schiff base and it's copper(II) complex will certainly enrich the molecular library having solvent-induced distortion in copper(II) complex with important catalytic and biological activities

## Declaration of Competing Interest

The authors declare that they have no known competing financial interests or personal relationships that could have appeared to influence the work reported in this paper.

## CRediT authorship contribution statement

**Subham Mukherjee:** Conceptualization, Formal analysis, Methodology, Investigation. **Chanchal Kumar Pal:** Formal analysis, Methodology, Investigation. **Muddukrishnaiah Kotakonda:** Formal analysis, Methodology, Investigation, Validation. **Mayank Joshi:** Formal analysis, Validation. **Madhusudan Shit:** Formal analysis, Methodology, Investigation. **Prasanta Ghosh:** Formal analysis, Visualization. **Angshuman Roy Choudhury:** Software, Validation. **Bhaskar Biswas:** Conceptualization, Writing – review & editing, Supervision.

## Acknowledgements

BB thanks Science and Engineering Research Board (SERB), India for financial support under Empowerment and Equity Opportunities for Excellence in Science (EEQ/2020/000079). The authors sincerely acknowledge the Department of Technology of Anna University, Chennai, India for supporting the measurement of biological activities.

## Supplementary materials

Supplementary material associated with this article can be found, in the online version, at doi:10.1016/j.molstruc.2021.131057.

## References

[1] S. Roy, M. Böhme, S.P. Dash, M. Mohanty, A. Buchholz, S.Majumder W.Plass, S. Kulanthaivel, I. Banerjee, H. Reuter, W. Kaminsky, R. Dinda, Inorg. Chem. 57 (2018) 5767–5781.
[2] W.A. Zoubi, Y.G. Ko, Appl. Organomet. Chem. 31 (2017) e3574.
[3] A. Shili, A. Ayadi, S. Taboukhat, N. Zouari, B. Sahraoui Conceptualisation, A. El-Ghayoury, J. Mol. Struct. 1222 (2020) 128933.
[4] King-Thom Chung, J. Environ. Sci. Health, part C 34 (2016) 233–261.
[5] H. Zollinger, Color Chemistry, Syntheses, Properties and Applications of Organic Dyes and Pigments, 3rd edition, Wiley-VCH, Weinheim, Germany, 2003.
[6] N.M. Aljamali, Biochem. Anal. Biochem. 4 (2015) 1000169.
[7] V.M. Dembitsky, T.A. Gloriozova, V.V. Poroikov, Nat. Prod. Bioprospect. 7 (2017) 151–169.
[8] S. Concilio, L. Sessa, A.M. Petrone, A. Porta, R. Diana, P. Iannelli, S. Piotto, Molecules 22 (6) (2017) 875.
[9] H. Nishihara, Coord. Chem. Rev. 249 (2005) 1468–1475.
[10] H.A. Wegner, Angew. Chem. Int. Ed. 51 (2012) 4787.
[11] H. Koshima, N. Ojima, H. Uchimoto, J. Am. Chem. Soc. 131 (2009) 6890.
[12] G. Heitmann, C. Schütt, R. Herges, Eur. J. Org. Chem. 22 (2016) 3817.
[13] A.D. Garnovskii, E.V. Sennikova, B.I. Kharisov, The Open Inorg, Chem. J. 3 (2009) 1–20.
[14] J. Valentová, S. Varényi, P. Herich, P. Baran, A. Bilková, J. Kozíšek, L. Habala, Inorg. Chim. Acta 480 (2018) 16.
[15] S. Al-Saeedi, L.H. Abdel-Rahman, A.M. Abu-Dief, S.M. Abdel-Fatah, T.M. Alotaibi, A.M. Alsalme, Catalysts 8 (2018) 452.
[16] E.L. De Araújo, H. Franciane, G. Barbosa, E.R. Dockal, É. Tadeu, G. Cavalheiro, Int. J. Biol. Macromol. 95 (2016) 168.
[17] W.J. Lian, X.T. Wang, C.Z. Xie, H. Tian, X.Q. Song, H.T. Pan, X. Qiao, J.Y. Xu, Dalton Trans 45 (2016) 9073.
[18] L.H. Abdel-Rahman, M.S.S. Adam, A.M. Abu-Dief, H. Moustafa, M.T. Basha, A.S. Aboraia, B.S. Al-Farhan, H. El-Sayed Ahmed, Appl. Organometal. Chem. 32 (2018) e4527.
[19] B. Iftikhar, et al., J. Mol. Struct. 1155 (2018) 337–348.
[20] E. Akila, M. Usharani, S. Vimala, R. Rajavel, Chem. Sci. Rev. Lett. 1 (2012) 181–194.
[21] S.E. Allen, R.R. Walvoord, R. Padilla-Salinas, M.C. Kozlowski, Chem. Rev. 113 (2013) 6234–6458.
[22] X. Liu, N.Novoa C.Manzur, S. Celedón, D. Carrillo, J. Hamon, Coord. Chem. Rev. 357 (2018) 144–172.
[23] P. Capdevielle, M. Maumy, Tetrahedron 57 (2001) 379.
[24] P.K. Mudi, R.K Mahato, M. Joshi, M. Shit, A.R. Choudhury, H.S. Das, B. Biswas, J. Appl. Organometal. Chem. 35 (2021) e6211.

[25] (a) S. Mukherjee, S. Roy, S. Mukherjee, B. Biswas, J. Mol. Struct. 1217 (2020) 128348; (b) A. Sańchez-Ferrer, J.N. Rodrıǵuez-Loṕez, V. Garcıá-Cańovas, F.G. Carmona, Biochim. Biophys. Acta 1 (1995) 1247.
[26] C. Gerdemann, C. Eicken, B. Krebs, Acc. Chem. Res. 35 (2002) 183.
[27] (a) F. Fusetti, K.H. Schro¨ter, R.A. Steiner, P.I. van Noort, T. Pijning, H.J. Rozeboom, K.H. Kalk, M.R. Egmond, B.W. Dijkstra, Structure 10 (2002) 259; (b) R.A. Steiner, I.M. Kooter, B.W. Dijkstra, Biochem 41 (2002) 7955; (c) I.M. Kooter, R.A. Steiner, B.W. Dijkstra, P.I. van Noort, M.R. Egmund, M. Huber, Eur. J. Biochem. 269 (2002) 2971.
[28] E.I. Solomon, D.E. Heppner, E.M. Johnston, J.W. Gins bach, J. Cirera, M. Qayyum, M.T. Kieber-Emmons, C.H. Kjaergaard, R.G. Hadt, L. Tian, Chem. Rev. 114 (2014) 3659.
[29] E.I. Solomon, M.J. Baldwin, M.D. Lowery, Chem. Rev. 92 (1992) 521.
[30] (a)E.I. Solomon, B.L. Hemming, D.E. Root, Electronic Structures of Active Sites in Copper Proteins: Coupled Binuclear and Trinuclear Cluster Sites in Bioinorganic chemistry of Copper, (K.D. Karlin, Z. Tyeklar), Chapman & Hall Publishing House, New York, USA, (1993) doi:10.1007/978-94-011-6875-5.; (b) C. Mukherjee, U. Pieper, E. Bothe, V. Bachler, E. Bill, T. Weyhermu¨ller, P. Chaudhuri, Inorg. Chem. 47 (2008) 8943.
[31] T. Punniyamurthy, S. Velusamy, J. Iqbal, Chem. Rev. 105 (2005) 2329.
[32] T. Punniyamurthy, L. Rout, Coord. Chem. Rev. 252 (2008) 134.
[33] K Selmeczi, M. Réglier, M. Giorgi, G. Speier, Coord. Chem. Rev. (2003) 19 2003.
[34] P.J. Walsh, M.C. Kozlowski, Fundamentals of Asymmetric Catalysis, University Science Books, Sausalito, CA, 2009 Chapter 8.
[35] S. Mahato, N. Meheta, K. Muddukrishnaiah, M. Joshi, M. Shit, A.Roy Choudhury, B. Biswas, Polyhedron 194 (2020) 114933.
[36] C. Duncan, A.R. White, Metallomics 4 (2012) 127.
[37] J. Zhang, D. Duan, J. Xu, J. Fang, ACS Appl. Mat. Interfer.c 10 (2018) 33010.
[38] K.Y. Djoko, M.M. Goytia, P.S. Donnelly, M.A. Schembri, W.M. Shafer, A.G. McEwan, Antimicrob. Agents Chemother. 59 (2015) 6444.
[39] B.S. Furniss, A.J. Hannaford, P.W.G. Smith, A.R. Tatchell, Vogel's Textbook of Practical Organic Chemistry, 1989, p. 952. Fifth Edition.
[40] CrysAlisPro 1.171.39.35cRigaku Oxford Diffraction, Rigaku Corporation, Tokyo, Japan, 2017.
[41] G.M. Sheldrick, SHELXT- Integrated space-group and crystal-structure determination, Acta Cryst. A71 (2015) 3.
[42] G.M. Sheldrick, Crystal structure refinement with SHELXL, Acta Cryst. C71 (2015) 3.
[43] O.V. Dolomanov, L.J. Bourhis, R.J. Gildea, J.A.K. Howard, H. Puschmann, J. Appl. Cryst. 42 (2009) 339.
[44] (a) L.I. Simandi, S. Nemeth, N. Rumlis, J. Mol. Catal. 42 (1987) 357; (b) Z. Szeverenyl, E.R. Mileava, L.I. Simandi, J. Mol. Catal. 67 (1991) 251; (c) G.C. Paul, K. Das, S. Maity, S. Begum, H.K. Srivastava, C. Mukherjee, Inorg. Chem. 58 (2019) 1782; (d) F. Benedini, G. Galliani, M. Nali, B. Rindone, S. Tollari, J. Chem. Soc. Perkin Trans. 2 (1985) 1963.
[45] (a) N.C. Jana, M. Patra, P. Brandão, A. Panja, Inorg. Chim. Act. 490 (2019) 163; (b) S. Thakur, S. Banerjee, S. Das, S. Chattopadhyay, New J. Chem. 43 (2019) 18747; (c) M. Garai, D. Dey, H.R. Yadav, A.R. Choudhury, M. Maji, B. Biswas, ChemistrySelect 2 (2017) 11040; (d) A. De, M. Garai, H.R. Yadav, A.R. Choudhury, B. Biswas, Appl. Organomet. Chem. 31 (2017) e3551.
[46] C.K. Pal, S. Mahato, H.R. Yadav, M. Shit, A.R. Choudhury, B. Biswas, Polyhedron 174 (2019) 114156.
[47] (a) B. Chowdhury, M. Maji, B. Biswas, J. Chem. Sci 129 (2017) 1627–1637; (b) A. De, D. Dey, H.R. Yadav, M. Maji, V. Rane, R.M. kadam, A.R. Choudhury, B. Biswas, J. Chem. Sci. 128 (2016) 1775–1782.
[48] (a) S. Khan, S. Herrero, R. Gonzalez-Prieto, M.G.B. Drew, S. Banerjee, S. Chattopadhyay, New J. Chem. 42 (2018) 13512; (b) T.M. Rajendiran, Transit. Met. Chem. 28 (2003) 447.
[49] A.S. Smirnov, L.M.D.R.S. Martins, D.N. Nikolaev, R.A. Manzhos, V.V. Gurzhiy, A.G. Krivenko, K.O. Nikolaenko, A.V. Belyakov, A.V. Garabadzhiua, P.B. Davidovich, New J. Chem. 43 (2019) 188.
[50] L.Z. Cai, W.T. Chen, M.S. Wang, G.C. Guo, J.S. Huang, Inorg. Chem. Commun. 7 (2004) 611–613.
[51] A. De, D. Dey, H.R. Yadav, M. Maji, V. Rane, R.M. kadam, A.R. Choudhury, B. Biswas, J. Chem. Sci. 128 (2016) 1775–1782.
[52] E.C.M. Ording-Wenker, M.A. Siegler, M. Lutz, E. Bouwman, Dalton Tran. 44 (2015) 12196.
[53] D. Dey, S. Das, H.R. Yadav, A. Ranjani, L. Gyathri, S. Roy, P.S. Guin, D. Dhanasekaran, A.R. Choudhury, M.A. Akbarsha, B. Biswas, Polyhedron 106 (2016) 106–114.
[54] P.K. Mudi, N. Bandopadhyay, M. Joshi, M. Shit, S. Paul, A.R. Choudhury, B. Biswas, Inorg. Chim. Acta 505 (2020) 119468.
[55] A. Reyes-Jara, N. Cordero, J. Aguirre, M. Troncoso, G. Figueroa, Front. Microbiol. 7 (2016) 626.
[56] H. Li, et al., Enhancing the antimicrobial activity of natural extraction using the synthetic ultra small metal nanoparticles, Sci. Rep. 5 (2019).